Jet Propulsion Laboratory
California Institute of Technology

Memorandum
IOM 343R-07-005
2 August 2007
Revised 22 February 2008

Planetary and lunar ephemeris DE418

W. M. Folkner, E. M. Standish, J. G. Williams, D. H. Boggs

Abstract

The planetary and lunar ephemeris DE418 was created for use by the New Horizons project in planning for the 2015 Pluto encounter. The Pluto observation sets used previously have been reduced with updated transformations to the IAU celestial reference frame, and have been augmented with new observations and a significant historical data set not used previously. The orbits of Earth and Mars have been updated with the most recent Mars spacecraft ranging and VLBI data, so DE418 is suitable for use by the Phoenix and other Mars projects. DE418 also represents the first combined solution with planetary and lunar laser ranging data in more than a decade, resulting in a significant improvement in the lunar orbit and physical librations relative to earlier planetary/lunar ephemerides.

1. Introduction

The planetary and lunar ephemeris DE418 is the successor to the previously released ephemeris DE414 (Standish 2006). DE418 is released specifically for the purpose of planning by the New Horizons project for the Pluto encounter in 2015. The Pluto orbit and its uncertainty have been extensively reanalyzed as described below. Some potentially interesting data have not yet been included due to time constraints, such as Hubble Space telescope observations and stellar occultations, but these are not expected to significantly affect the position and uncertainty predicted for 2015. Ground-based astrometric observations are increasingly accurate, especially since the release of the Hipparcos star catalog, and serve to determine the current right ascension and declination. However determination of the distance from Earth to Pluto, and the prediction of its position in the future, rely on the determination of all six orbital elements. Since Pluto has been observed for less than half of its orbital period, the orbit is poorly determined relative to the other planets. Of the six orbital elements, the semi-major axis and eccentricity are particularly poorly determined and more dependent upon the length of the observation set. Thus an emphasis has been placed on observations for as long a period of time as possible. The observation sets and residuals are described in Section 5 along with an analysis of the uncertainty.

The orbits of Earth and Mars are continually improved through measurements of spacecraft in orbit about Mars. DE414 was fit to Mars spacecraft range data through the first quarter of 2005 and VLBI measurements of Mars spacecraft through 2003. The orbit of Mars (and to a lesser extent Earth) are significantly perturbed by asteroids, impacting the predicted uncertainty of the Mars and Earth orbits. The addition of new data is necessary to update the orbit estimates and, hopefully, to allow the estimation of the asteroid masses to improve orbit prediction accuracy. DE418 incorporates range data through the end of 2006. VLBI (Delta-DOR)

observations of Mars spacecraft were resumed in January 2006 for the purpose of improving the Mars orbit for the MSL project. VLBI data through June 2007 have been included in the DE418 estimate. The estimation of asteroid masses has been done differently than for DE414. For DE414 the masses of the 67 most significant asteroids were estimated with constraints based on knowledge of the asteroid diameters and probable densities. For DE418 the number of asteroid masses estimated was reduced to a selected subset of 12 asteroids. There is some evidence that this change in estimation procedure will lead to an improved orbit prediction, though there is still room for improvement.

DE418 is the first ephemeris since DE403, made in 1995, to simultaneously fit planetary observations and lunar laser ranging observations. For ephemerides in between DE403 and DE418 the lunar orbit was constrained to the DE403 lunar orbit in various ways. DE418 thus incorporates 12 more years of lunar data than its predecessors. For DE418 the number of lunar parameters included in the fit was reduced to simplify the combination with the planetary data, but they fit the lunar laser ranges quite well. Thus the lunar orbit, and physical librations on DE418 are significantly improved relative to DE414 or DE405.

With the exception of Saturn, the orbits of planets other than Pluto and Mars on DE418 were estimated with same process and data as used for DE414. Orbit differences between DE418 and DE414 for those planets are characteristic of the uncertainties in the orbits. For Saturn, DE418 was fit to estimated right ascension, declination, and distance to Earth for each orbit of the Cassini spacecraft about Saturn (Jacobson 2007). This results in a significant change to the orbit of Saturn and fits the Cassini observations quite well. However a detailed analysis of the combination of the other observations with the Cassini data has been deferred to the future.

2. Time and mass constants

For the ephemeris DE418, as with all previous JPL ephemerides, the positions of the moon and planets are integrated in a solar-system barycentric coordinate system (e.g. Moyer 2000) with a coordinate time which runs roughly at the same rate as atomic time on Earth. In a resolution adopted by the International Astronomical Union in 2006, the time scale TDB (Temps Dynamique Barycentrique, Barycentric Dynamical Time) was defined to be consistent with the JPL ephemeris time. The relationship used to convert planetary observations times (in UTC and TAI) to coordinate time have been done using the formulation of Fairhead and Bretagnon (1990), which is consistent, for planetary navigation accuracies, with the simpler approximation given in Moyer (2000). The Moyer dot product formulation was used for analyzing the lunar ranges.

For historical reasons, the positions of the planets are integrated in spatial units of astronomical units and time in (TDB) days, with the product of the gravitation constant G and mass of the sun, GM_{sun}, held fixed. In the reduction of the data, with the speed of light defined in m/s and light-times measured in seconds, the scale factor for the length of the AU in km is estimated. The GM_{sun} value can then be converted from AU^3/day^2 to km^3/s^2 using this AU scale parameter. The GM values of the planets are best determined in km^3/s^2, and are then converted to AU^3/day^2 for the ephemeris integration. Since the orbits of the Earth and Mars about the Sun are determined with increasing accuracy by ranging to Mars spacecraft, the AU estimate is continually updated. Thus, a fully converged ephemeris requires multiple iterations with conversions of the masses of the planets into internal units. For DE418, due to time constraints, this process has not completely converged and the masses used in the integration are slightly different than the current best estimates. This does not reduce the accuracy of the estimation of

the relative positions of the planets during and near to the time of the data fit, but might affect the projections into the distant past or affect analysis of solar system parameters such as system angular momentum. For that reason it is not recommended that DE418 be used for projections beyond the time span for which it is integrated (1900-2050) and it should be used with caution for purposes other than spacecraft navigation.

The GM values given within the DE418 file are listed in Table 1 below. The GM of the Earth-Moon system (GMB) is determined by a separate, more complete fit to lunar laser ranges. The Earth-Moon mass ratio, and the AU scale, equivalent to GM of the Sun in km^3/s^2, were estimated in the creation of DE418. We caution that tabulated GM values in km^3/s^2 depend on a solar system barycentric formulation using TDB; GM_{earth} will not exactly match earth-satellite-derived values based on a geocentric analysis. For the convenience of NASA planetary navigation teams, the masses of the other planets are consistent with the current best estimates of the planets, which are slightly different than those used in the DE418 integration. For planets with satellites (moons), the GM values listed are for the total planetary system, including satellites. (The positions on the planetary ephemeris are for the barycenter of those planetary systems.) This allows users of the navigation software to use the most current estimates of planetary gravity fields more easily (since some software uses as default the mass of the planet listed on the ephemeris file in the computation of the effects of the gravity field). The GM values for Mars and Pluto are also the same as those used in the most recent satellite ephemerides.

Table1: GM values of planetary bodies/systems included in DE418 file header

Body/System	GM (km^3/s^2)	GM_{sun}/GM_{planet}	Reference
Mercury	22032.090000	6023597.399977	Anderson et al [1987]
Venus	324858.592000	408523.718653	Konopliv et al. [1999]
Earth	398600.436200	332946.048191	DE418 fit
Mars	42828.375210	3098703.590536	Konopliv et al. [2006]
Jupiter	126712764.800000	1047.348625	Jacobson et al. [2005]
Saturn	37940585.200000	3497.901768	Jacobson et al. [2006]
Uranus	5794548.600000	22902.981613	Jacobson et al. [1992]
Neptune	6836535.000000	19412.237345	Jacobson et al. [1991]
Pluto	977.000000	135836683.766690	Jacobson et al. [2007]
Sun	132712440040.056500	1.000000	DE418 fit
Moon	4902.800107	27068703.017324	DE418 fit
Earth-Moon	403503.236307	328900.559150	LLR fit

3. Mars measurement analysis

For DE418, the orbits of the Earth-Moon barycenter and Mars, and the Earth-Moon mass ratio, were estimated from range and VLBI measurements from the two Viking landers, the Mars Pathfinder lander, and the MGS, Odyssey, and MRO orbiters. The Doppler data from the Viking and Pathfinder landers was used in the DE414 fit to estimate Mars rotation. A more accurate Mars rotation can now be estimated at the same times as estimation of the gravity field by combing the lander Doppler with orbiter Doppler (Konopliv et al. 2006). Thus the Viking lander

and Mars Pathfinder Doppler data were not included in the DE418 solution, and the Mars rotation model was adopted from Konopliv.

The DE414 ephemeris integration included the effects of 67 asteroids with individual masses and 276 asteroids whose masses are defined by three density classes. For DE414 the density of each class and the masses of each of the 67 individual masses were estimated with constraints. This technique allowed all of the range measurements to be fit, but does not necessarily predict future range measurements well. Figure 1 shows a plot of Odyssey measurements relative to DE414. The DE414 fit included range measurements through March 2005. As can be seen, over the next year the residuals of range measurements to data not included in the fit grew fairly quickly beyond 20 m. For an intermediate ephemeris prior to DE418 the masses of 12 individual asteroids were estimated without constraints using data through the end of 2005. The set of asteroid masses was selected to keep the residuals of the unfit range measurements in 2006 and 2007 small, as shown in Figure 2. For the final DE418 all range measurements through 2007 were included in the estimation procedure and the resulting masses were consistent with those estimated with the shorted data arc. Figure 3 shows the Mars spacecraft ranging residuals against DE418. Clearly the data from Odyssey and MRO since the start of 2007 are not fit as well as had been hoped. A further development of the asteroid modeling will be pursued in the next several months in the development of a new ephemeris to be used for the Phoenix approach to Mars.

Figures 4 and 5 show the residuals of Mars spacecraft VLBI measurements included in the DE418 estimation. The measurements made in 2006 and 2007 show good accuracy, with a few exceptions. The average VLBI residual is 0.25 milli-arcsecond (1.2 nanoradian) on the Goldstone-Madrid baseline (essentially right ascension) and 0.5 milli-arcsecond (2.5 nanoradian) for the Goldstone-Australia baseline (essentially an average of right ascension and declination). The measurements tie the ephemeris DE418 directly to the ICRF frame defined by extra-galactic radio sources to an accuracy better than 0.5 milli-arcsecond (2.5 nanoradian).

Figure 6 shows the difference in the Earth-Mars vector between DE418 and DE414. The differences are less than 0.5 km for the period 1990-2020, with a 0.4 km amplitude periodic difference in ecliptic latitude due to the addition of new VLBI data and the drifts in longitude and distance due to differences in asteroid mass estimation.

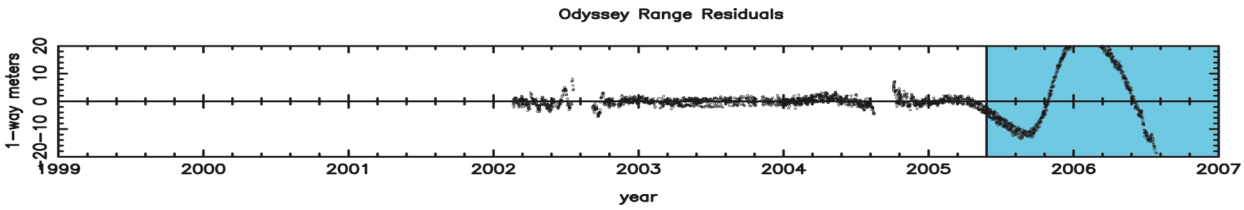

Figure 1: Mars Odyssey ranging residuals relative to DE414.

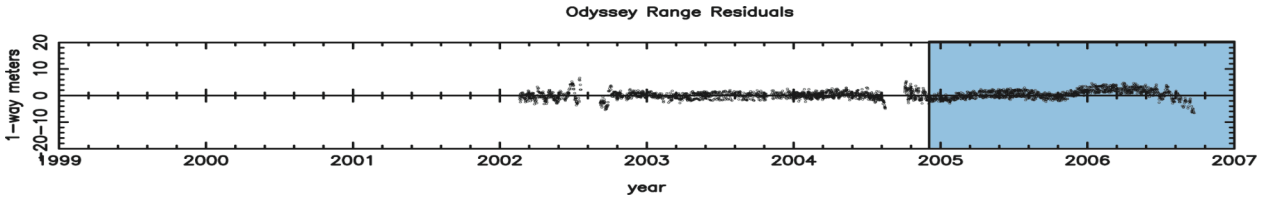

Figure 2: Mars Odyssey residuals relative to an intermediate ephemeris fit data through end of 2005 with fewer estimated asteroid masses.

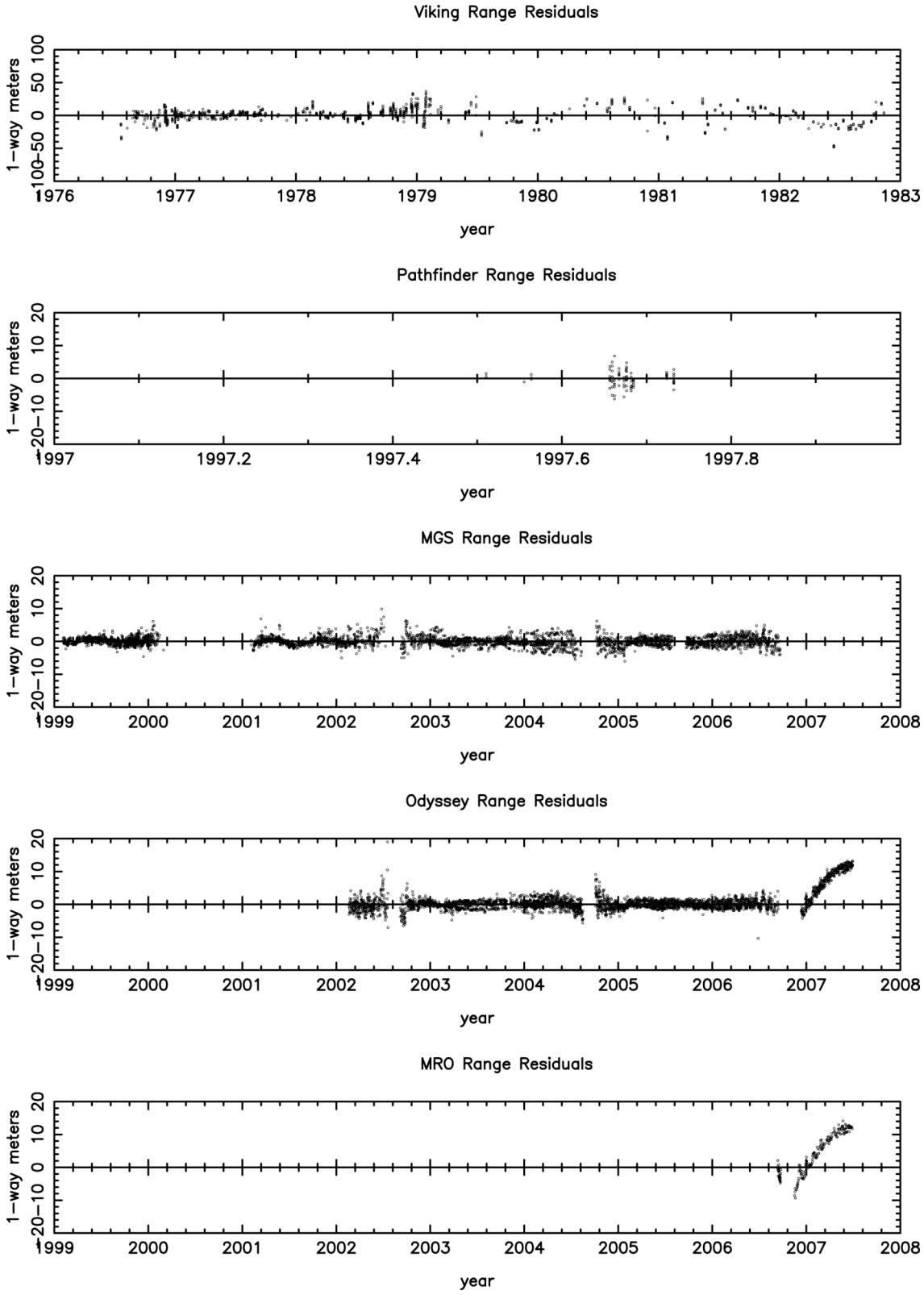

Figure 3: Mars spacecraft ranging residuals relative to DE418. Measurements made since the start of 2007 were not included in the DE418 estimation process.

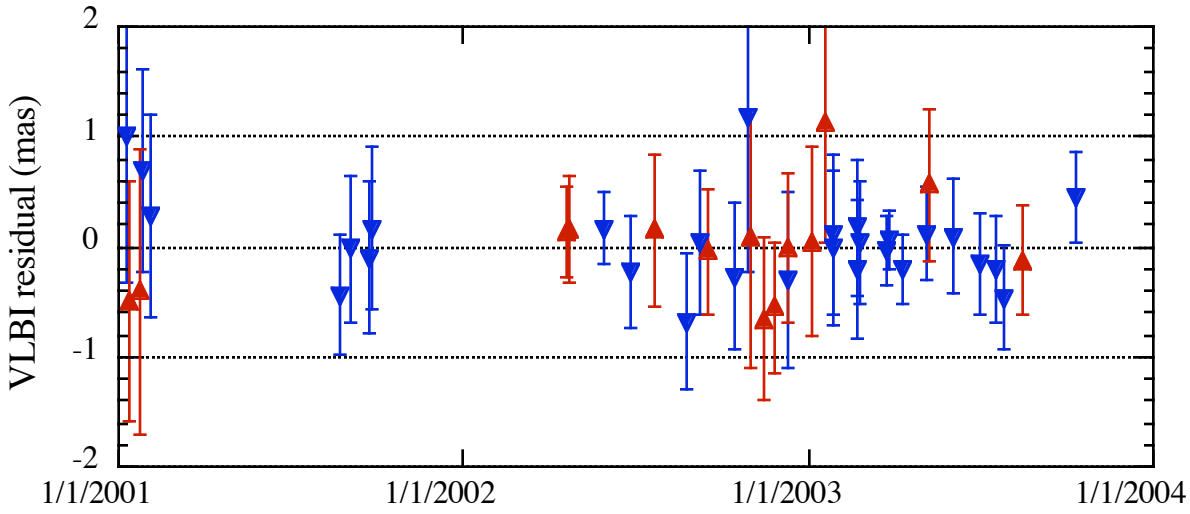

Figure 4: Residuals of Mars spacecraft VLBI observations relative to DE418 for the Goldstone-Madrid baseline (red) and Goldstone-Canberra baseline (blue) over the interval 2001 through 2003.

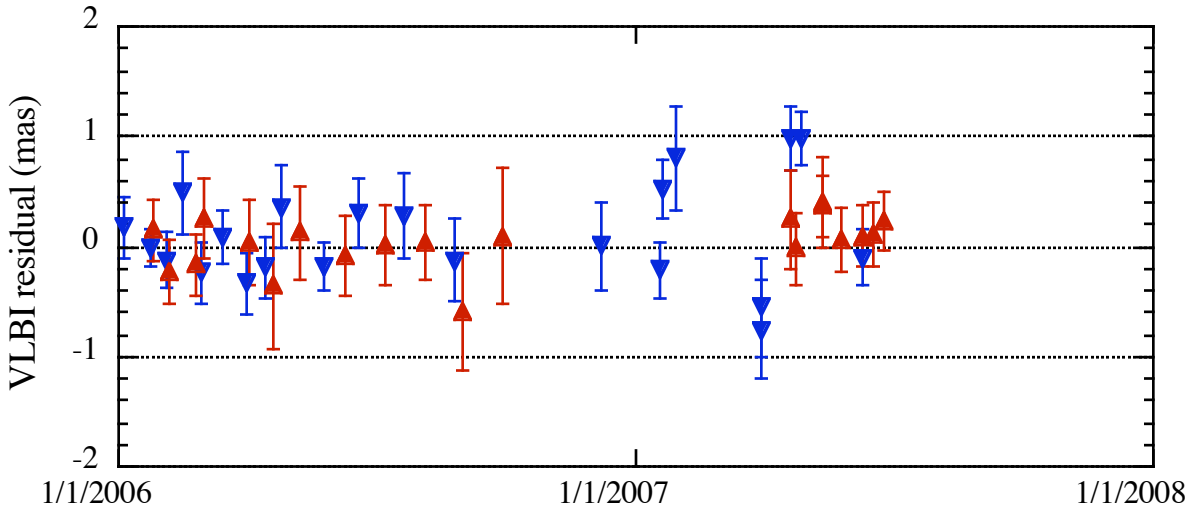

Figure 5: Residuals of Mars spacecraft VLBI observations relative to DE418 for the Goldstone-Madrid baseline (red) and Goldstone-Canberra baseline (blue) over the interval starting in 2006.

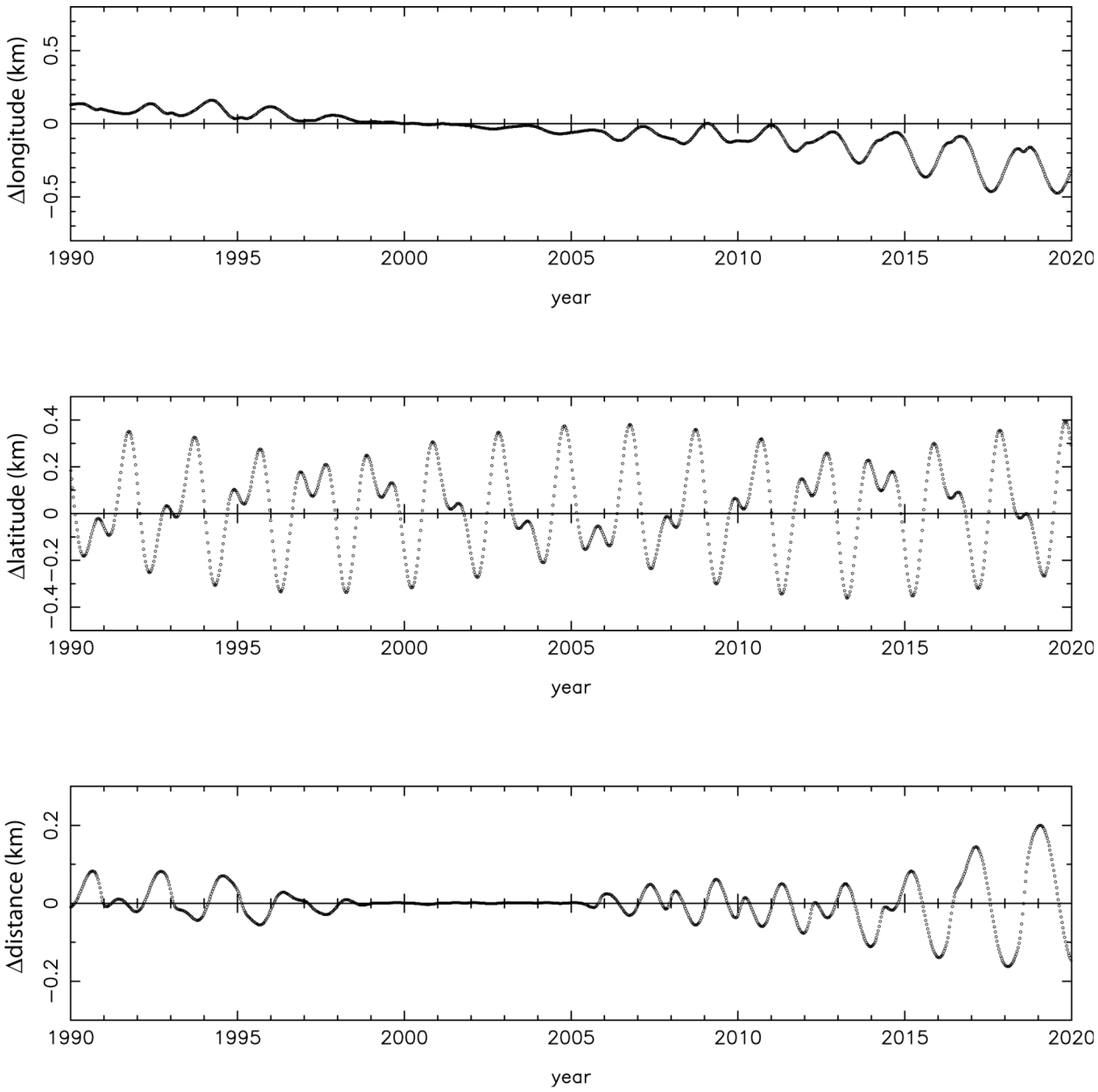

Figure 6: Difference in the Earth-Mars vector, in ecliptic coordinates, between DE418 and DE414.

4. Lunar Orbit and Orientation

The initial conditions for the lunar ephemeris and three dimensional lunar orientation (Euler angles and spin rates) were estimated in the fit to lunar laser ranging (LLR) data. A total of 16,471 ranges extend from March 16, 1970 to May 29, 2007. Modern range accuracies are an order-of-magnitude better than early data. Ranges were processed from McDonald Observatory (Texas), Observatoire de la Côte d'Azur (France), Haleakala Observatory (Hawaii), and Apache Point Observatory (New Mexico). The models for both the computation of the acceleration of the Moon in its orbit, for the numerical integration, and the computation of range, for the fits, depend on geophysical processes on the Earth and Moon.

For the Moon's gravity field, S_{31}, S_{33}, and all fourth-degree spherical harmonic coefficients were taken from the spacecraft-derived LP150Q set for spherical harmonics (Konopliv 2006). The remaining five third-degree coefficients were taken from a previous LLR solution. The lunar radius used with the gravity field was 1738 km. The estimated mass of the Moon depends on the Earth/Moon mass ratio and the GM of the Earth-Moon system (GMB). The mass ratio was estimated based largely on Mars spacecraft range data. The GMB, two lunar moment of inertia differences, Love numbers k_2 and h_2, dissipation parameters for tides and fluid core, oblateness of the fluid core/solid mantle interface and initial values for the fluid core orientation were taken from a previous LLR solution. The moment of inertia of the fluid core was set to $6x10^{-4}$ of the total moment and Love number l_2 was fixed at a model value of 0.0106. The static J_2 coefficient was based on the LP150Q value, but an adjustment was made for the constant J_2 tide contribution calculated from the difference between the LP150Q k_2 and the value used here. C_{22} was calculated from J_2 and the two moment of inertia differences. The lunar orientation (physical libration) initial conditions and retroreflector coordinates for Apollo 11, 14, 15 and Lunokhod 2 were estimated in the DE418 fit.

For the Earth's gravity field, J_3 and J_4 were taken from the GGM02C gravity field and the equatorial Earth radius used with gravity was set to 6378.1363 km. The J_2 coefficient was based on the GGM02C "tide free" value, but it was adjusted for a different Love number k_{20}. The tidal gravity model used three Love numbers k_{20}, k_{21}, and k_{22} with three tidal time delays for the long period (zonal), diurnal, and semidiurnal tides, respectively. The three Love numbers and the zonal (long period) time delay were from combined Earth and ocean tides. The tides change with frequency and values were chosen to approximately match the Mf, O1, and M2 tides, which are the most important tides in each of the three frequency bands for the tidal secular acceleration of the Moon. The zonal time delay was based on the FES2004 Mf ocean tide (Lyard et al. 2006; Ray 2006), but the diurnal and semidiurnal time delays were estimated. The computation of the range depends on the coordinates of the ranging stations which were estimated. Two rotation angles at J2000 were estimated to orient the Earth in space. The obliquity rate was also estimated, but the precession rate was based on a previous LLR solution. Several nutation coefficients were based on the IERS conventions as were the diurnal and semidiurnal UT1 terms, but the 18.6 yr nutation term came from an earlier LLR solution. Station motion was based on a previous LLR solution.

Figure 7 shows the difference in the Earth-Moon orbit between DE403 and DE418 over the two-year interval starting in January 2000. Differences of about two meters in amplitude are seen and largely represent the error in the predicted values based on the shorter data span in DE403.

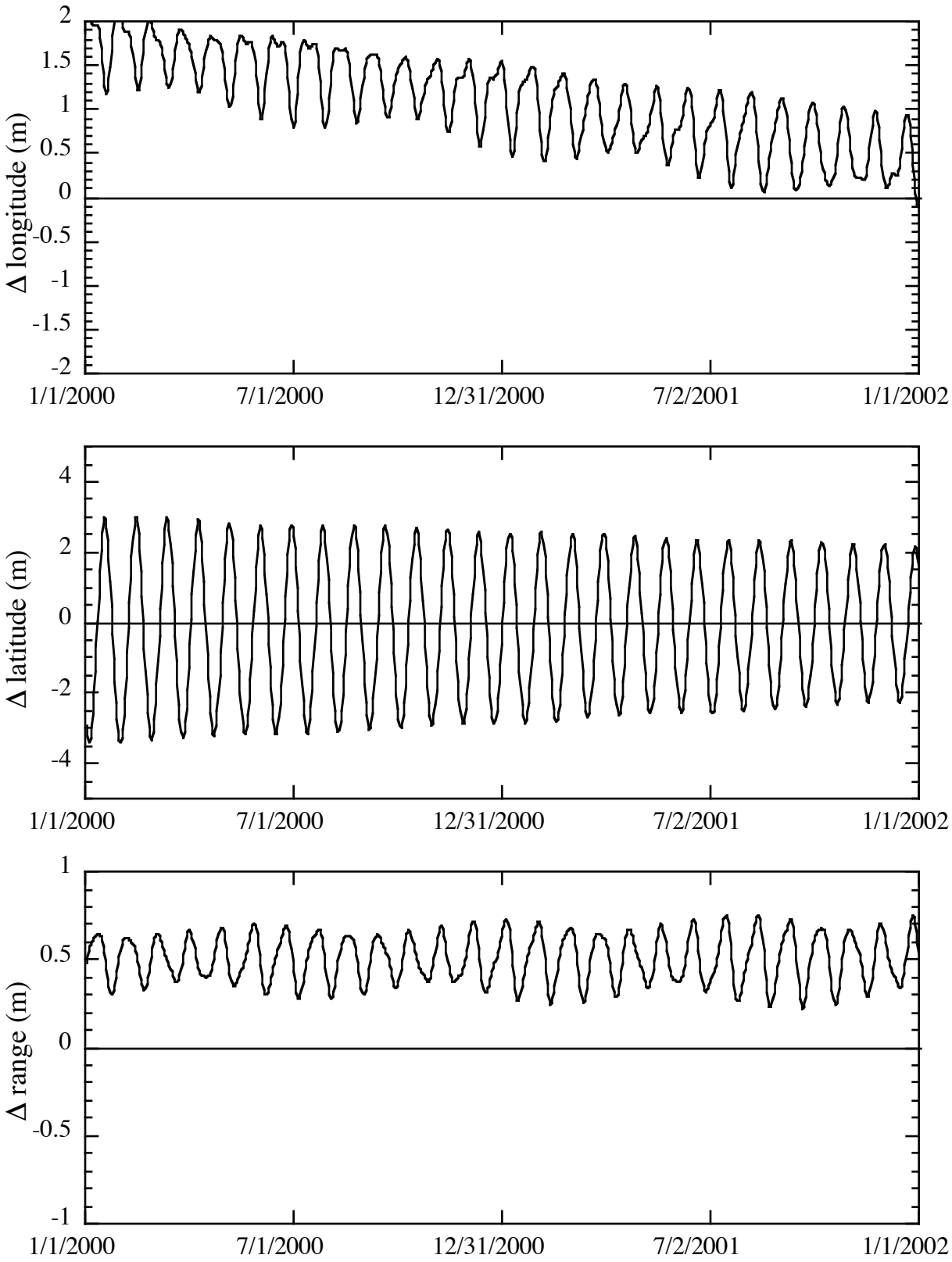

Figure 7: Difference in lunar orbit between DE418 and DE403.

5. Pluto measurement and uncertainty analysis

The orbit of Pluto is achieved by a fit to Earth-based observations of its right ascension and declination. DE418 has been fit to observations from 1914 (before its discovery) through June 2007. These observations cover less than one-half of the Pluto orbit period (248 years). This makes the determination of the orbit semi-major axis and eccentricity not very robust and very dependent on the data quality and relative weighting of different data sets. Systematic errors in the data are expected since they have been taken by a variety of observers using different instruments and different star catalogs over the century of observations.

For the ground-based astrometric measurements of Pluto, the planet and major satellite Charon are not resolved. The center of the observed image has been estimated to be 0.154 of the distance from Pluto to Charon in the plane of the sky (Elliot 2002).

Since 1995 there have been a series of very good observations of the position of Pluto referred to the IAU Celestial Reference frame, enabled by advances in instrumentation and by the Hipparcos star catalog. Figure 8 shows the measurement residuals for three sets of modern observations relative to the DE418 fit; from the US Naval Observatory in Flagstaff, Arizona (e.g. Stone et al. 2003); from the Table Mountain Observatory (Owen 2006); and from the CCD meridian instruments of Bordeaux and Valinhos (Rapaport et al. 2002). As seen in Figure 8, all three of these data sets are consistent and fit the orbit in DE418 very well, with RMS residuals less than 0.11 arcsecond. While there are other observations available for this time period, it will be seen that further reducing the uncertainty in right ascension and declination over this time period would not greatly help the uncertainty in the Pluto position predicted for 2015. Additional measurements may not be independent in any case, since they are subject to some common systematic errors, such as the accuracy of the Hipparcos star catalog and its tie to the ICRF.

From the late 1960's through 1990 there were a number of sets of observations of Pluto at a variety of institutions. Transformations for most of the star catalogs used for these Pluto observations to the ICRF have been computed by comparison with the Hipparcos catalog by Schwan (2001). We chose here to exclude data based on catalogs for which Schwan did not compute transformations to the ICRF. Figure 9 shows residuals of measurements by; Barbieri et al. (1972, 1975, 1979, 1988); Gemmo et al. (1994); Jenson (1979); Klemola and Harlan (1982, 1984, 1986); and Zappala et al. (1980, 1983). These residuals show larger scatter than the modern data, and some of the data sets show systematic trends which are not consistent between the data sets.

Observations from the period 1930-1970 are considered most important for the purpose of characterizing the uncertainty in the Pluto orbit at the time of the New Horizons encounter, because they, along with the modern data, define the length of the arc covered by reasonably good data. There are three data sets considered, only two of which are independent. A series of observations from Lowell, Yerkes, and McDonald observatories was reduced by G. Van Biesbroeck and published by Cohen et al. (1967). These were reduced against the FK3 star catalog. These have been transformed to the ICRF by values given in Schwan (2001) with residuals relative to DE418 shown in Figure 10. The residuals are fairly well behaved though small but significant drifts in right ascension and declination can be seen. Since measurements tend to be grouped at times of Pluto opposition (seen more clearly in Figure 8), Sharaf and Budnikova (1964) averaged measurements from each opposition into a single normal point. These normal points included much of the data from Lowell, Yerkes, and McDonald from

Figure 10. The residuals for these normal points are shown in Figure 11. The residuals are somewhat different in bias and slope than those of Figure 10, though consistent within the data scatter. Cohen et al. (1967) used both the individual points and the normal points in their fit to the Pluto orbit. For JPL ephemerides done through DE414 a similar process was followed. Since there are many fewer normal points, the individual points from Lowell, Yerkes, and McDonald tend to dominate the early data in those fits.

A separate series of Pluto observations from the Pulkovo astrograph covering the period 1930 to 1992 were published by Rylkov et al. (1995). These were reduced by the authors to the FK5 star catalog. For DE418 these were then converted to the ICRF using the formulation of Schwan (2001). The residuals of these measurements relative to DE418 are shown in Figure 12. These residuals show slightly lower scatter than the Sharaf and Budnikova points, and have the advantage of continuing nearly up to the modern era.

The final set of observations used in the DE418 fit are the pre-discovery data. Right ascension and declination were measured from images of star fields containing Pluto prior to its discovery (Sharaf and Budnikova, 1964). As shown in Figure 13, the residuals of these observations relative to DE418 have much larger scatter than the post-1930 data.

For creating the DE418 ephemeris, we decided to include the Pulkovo data and the Sharaf and Budnikova data weighted at their post-fit RMS scatter. The individual observations from Lowell, Yerkes, and McDonald were not included as they were not considered to be independent from the Sharaf and Budnikova normal points. The normal points were preferred since they are fewer in number so the scatter was felt to be more consistent with the true data noise. The modern data were included as individual observations and weighted at their data scatter. While this may be too optimistic, since their time span is short they do not dominate the expected uncertainty in the Pluto orbit for the 2105 New Horizons encounter. The pre-discovery observations were included in the fit weighted at their RMS level but do not affect the solution much. Finally the data from 1968 through 1990 (Figure 9) were included at their RMS scatter except that the Barbieri et al. data were somewhat de-weighted due to the relatively large number of individual observations and a fairly significant trend in the residuals.

Figure 14 shows the difference in the Pluto position (relative to the solar system barycenter) between DE418 and DE414. The differences are partly due to the addition of the Pulkovo observations and partly due to changes in the transformations of data to the ICRF frame and changes in the weighting of the data.

In order to estimate the uncertainty in the DE418 Pluto orbit, three test ephemerides were generated with different data sets, and the differences compared with the formal uncertainties. Figure 15 shows the difference between the three test ephemerides and DE418 (‘Nominal’). For the ephemeris labeled ‘Rylkov’ the Sharaf and Budnikova normal points were excluded from the fit, with all other data weights kept the same as the nominal. For the test ephemeris labeled ‘Sharaf’’ the Pulkovo data were excluded from the fit, with all other data weights kept the same as the nominal. For the test ephemeris labeled ‘Cohen’ the Pulkovo data and the Sharaf and Budnikova normal points were excluded from the fit, instead including the individual observations from Lowell, Yerkes, and McDonald weighted at their RMS times a scaling factor to account for the larger number of individual observations. Over the period 1990-2015 the three solutions are generally within 2000 km of the DE418 value for distance (which is inferred from

the long arc fit), about 1000 km in right ascension and about 750 km in declination. Note that an angular change of 0.01 arcsecond corresponds to about 3000 km at the distance to Pluto.

Figure 16 shows the formal uncertainty resulting from the least-squares fits for DE418 and for the three test ephemerides. Formal uncertainties in right ascension and distance are much larger at 2015 than at 1990, whereas the differences in the test ephemerides and DE418 are more symmetric over that time span. The largest formal uncertainty of the three test ephemerides is the 'Sharaf' case, since there are fewer normal points from Sharaf and Budnikova than Pulkovo observations, and the 'Cohen' test ephemeris data weights were adjusted to give about the same formal uncertainty as the nominal DE418 case. At 2015 the formal uncertainty in right ascension, declination, and distance are about 750 km, 300 km, and 1500 km respectively. The declination formal uncertainty thus seems too small by about a factor of two compared with the test ephemerides differences. The formal uncertainties in right ascension and distance appear to be a factor of about $\sqrt{2}$ too small compared with the test ephemerides differences relative to the nominal DE418.

Figure 16 also shows the formal uncertainty of the Pluto orbit estimated with only the modern data (1995-2007). Note that the formal uncertainty in right ascension and distance for times earlier than 1995 or later than 2005 with only the modern data taken into account is much larger than any of the other cases considered. This is consistent with those parameters being dependent on the orbit semi-major axis and eccentricity which are poorly determined from a data arc much shorter than the orbit period. Thus the uncertainty in the estimated distance to Pluto is not likely to improve much prior to the New Horizons encounter. The uncertainty in right ascension and declination will definitely improve with astrometric observations between now and the encounter.

Thus in assessing at this time the uncertainty of where Pluto will be in 2015, we recommend that the New Horizons project use an uncertainty of twice the formal uncertainty (in sigma), since otherwise the declination uncertainty in particular would be too optimistic. We assume that this is the case of most interest to the project at this time. Table 2 below gives a covariance for Pluto which has been scaled to the recommend values. The uncertainty in the Pluto ephemeris is so large compared with the Earth orbit uncertainty that the correlations are best approximated as zero. If the New Horizons project would like to include an Earth orbit uncertainty, we include in Table 3 a current Earth orbit uncertainty covariance (Folkner 2006).

If the project planning could take into account that a future ephemeris, in the 2010-2012 time frame, would be able to include Pluto observations much closer to the encounter time, then we would recommend using an uncertainty of about 1.5 times the formal uncertainty of DE418. The smaller factor would be sized more to account for the distance uncertainty. In either case the distance uncertainty will be the largest component of the total uncertainty ellipsoid.

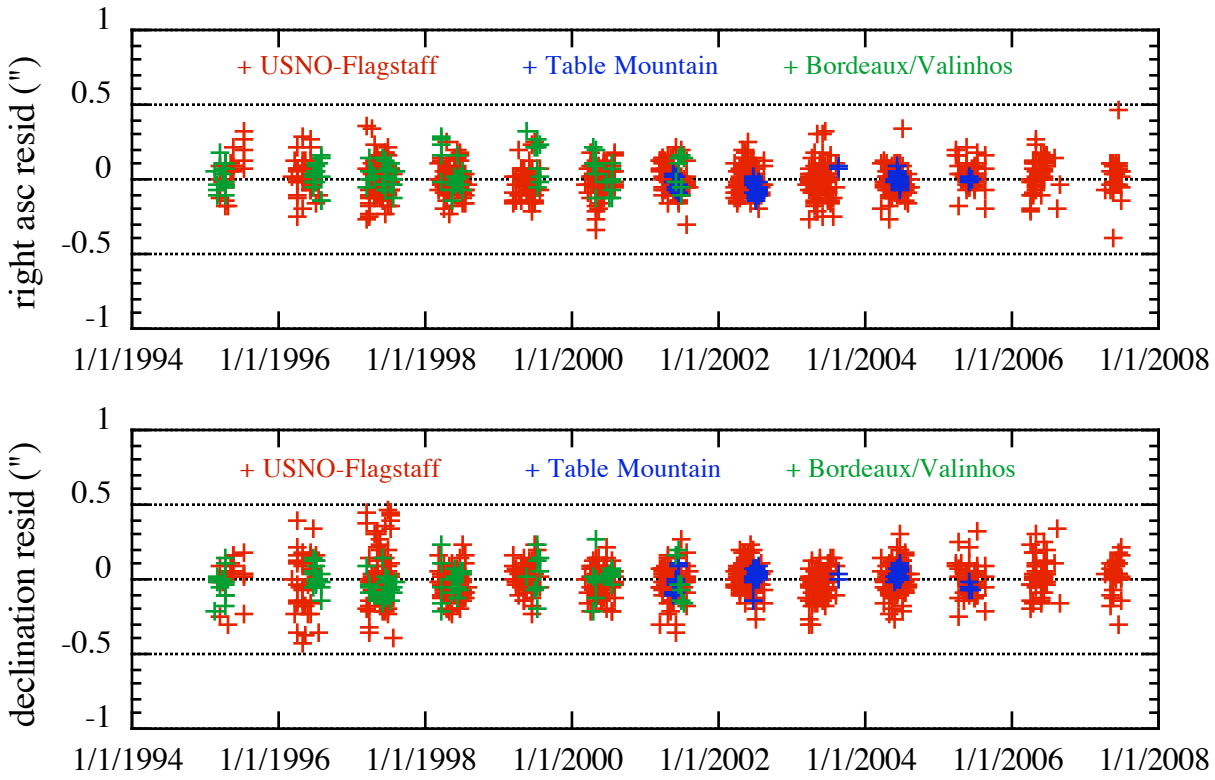

Figure 8: Residuals of modern Pluto observations relative to DE418.

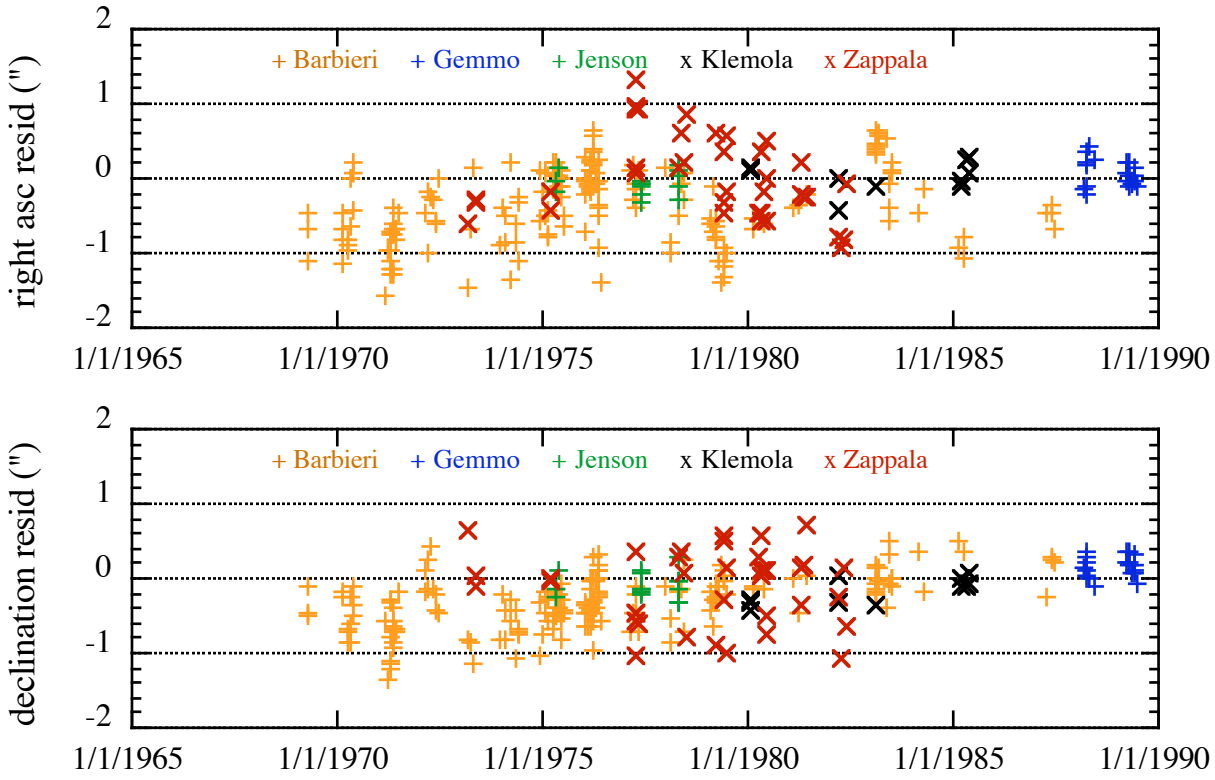

Figure 9: Residuals of Pluto observations made 1968-1990 relative to DE418.

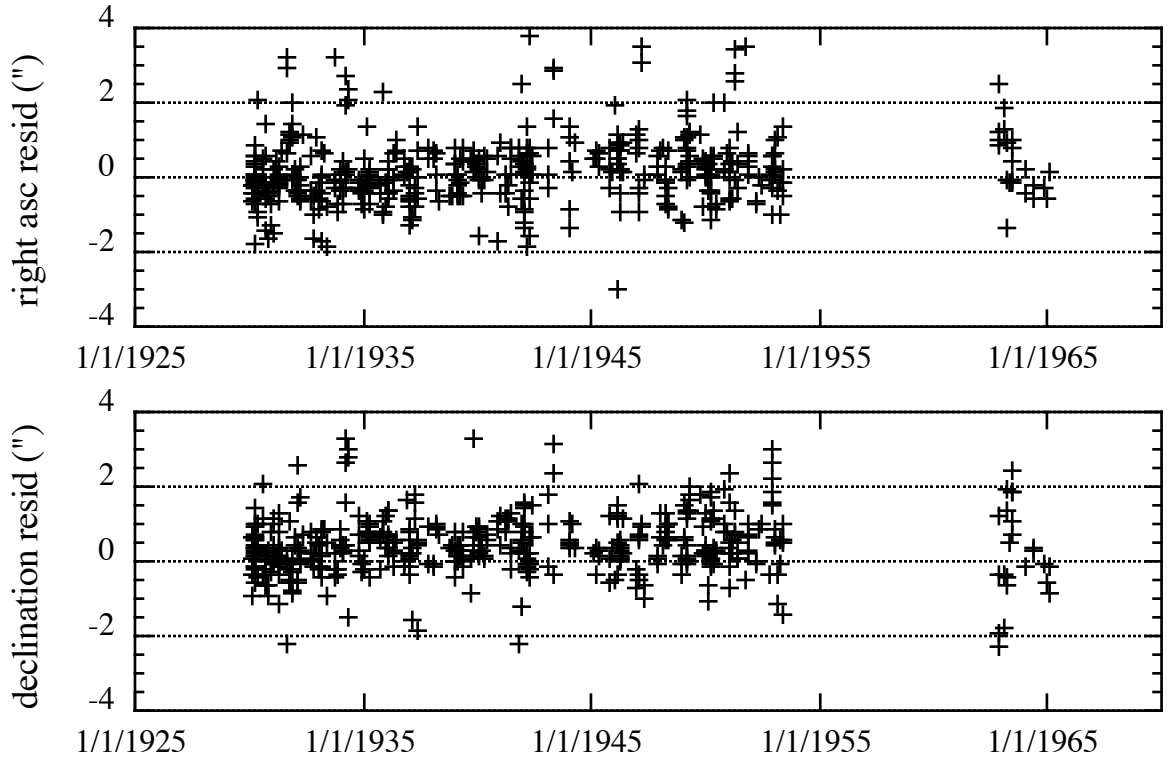

Figure 10: Residuals of Pluto observations made at Lowell, Yerkes, and McDonald, published in Cohen et al. (1967) relative to DE418.

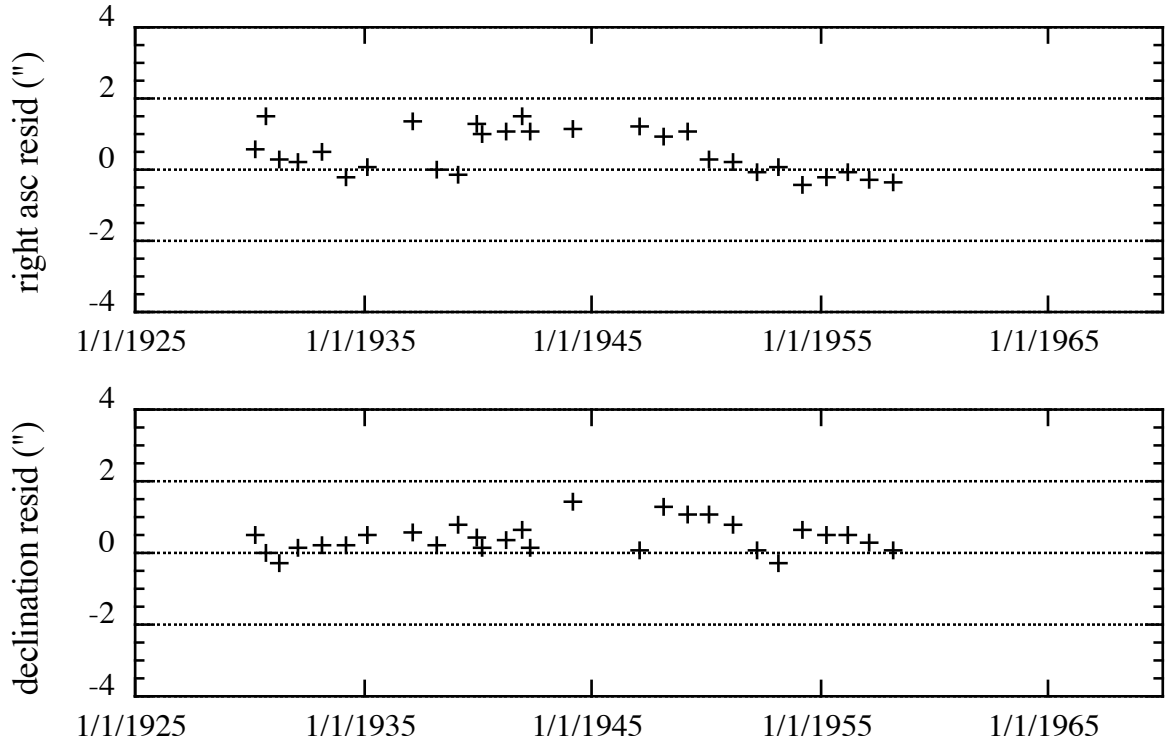

Figure 11: Residuals of Pluto observations reduced by Sharaf and Budnikova (1964) relative to DE418.

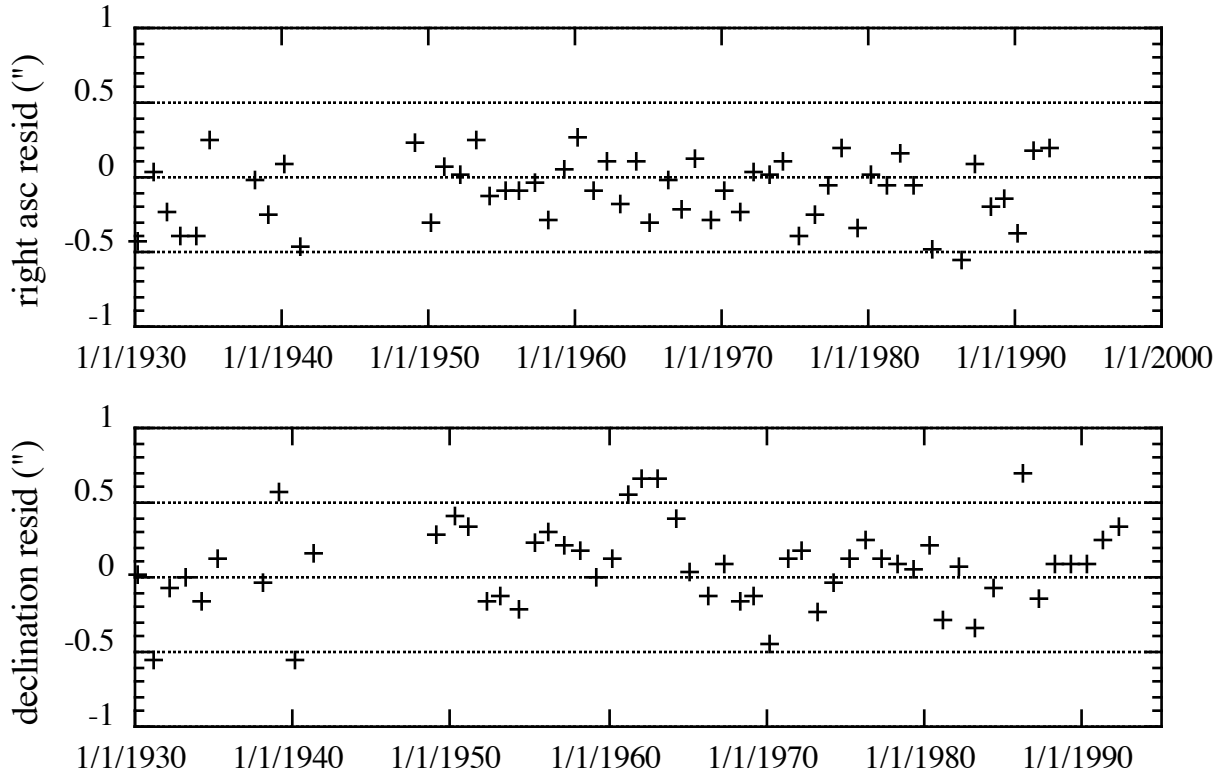

Figure 12: Residuals of Pluto observations from the Pulkovo astrograph relative to DE418.

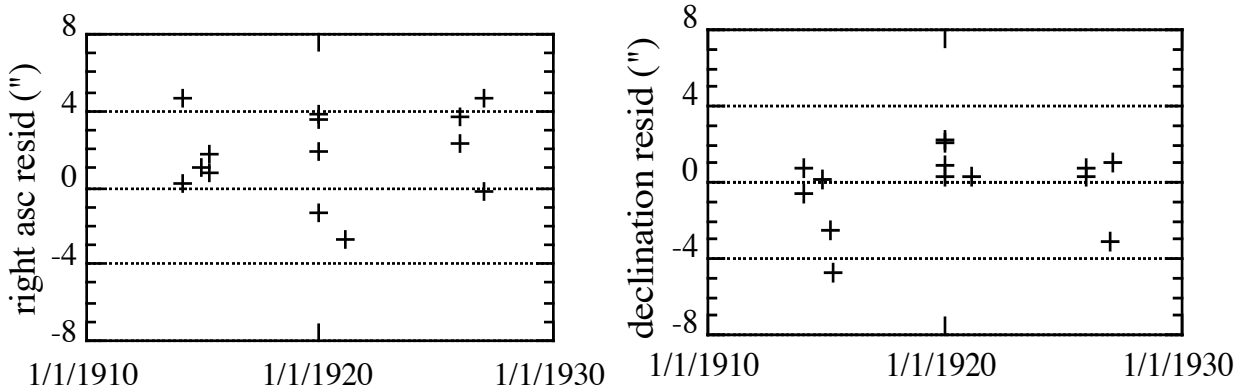

Figure 13: Residuals of Pluto observations prior to its discovery relative to DE418.

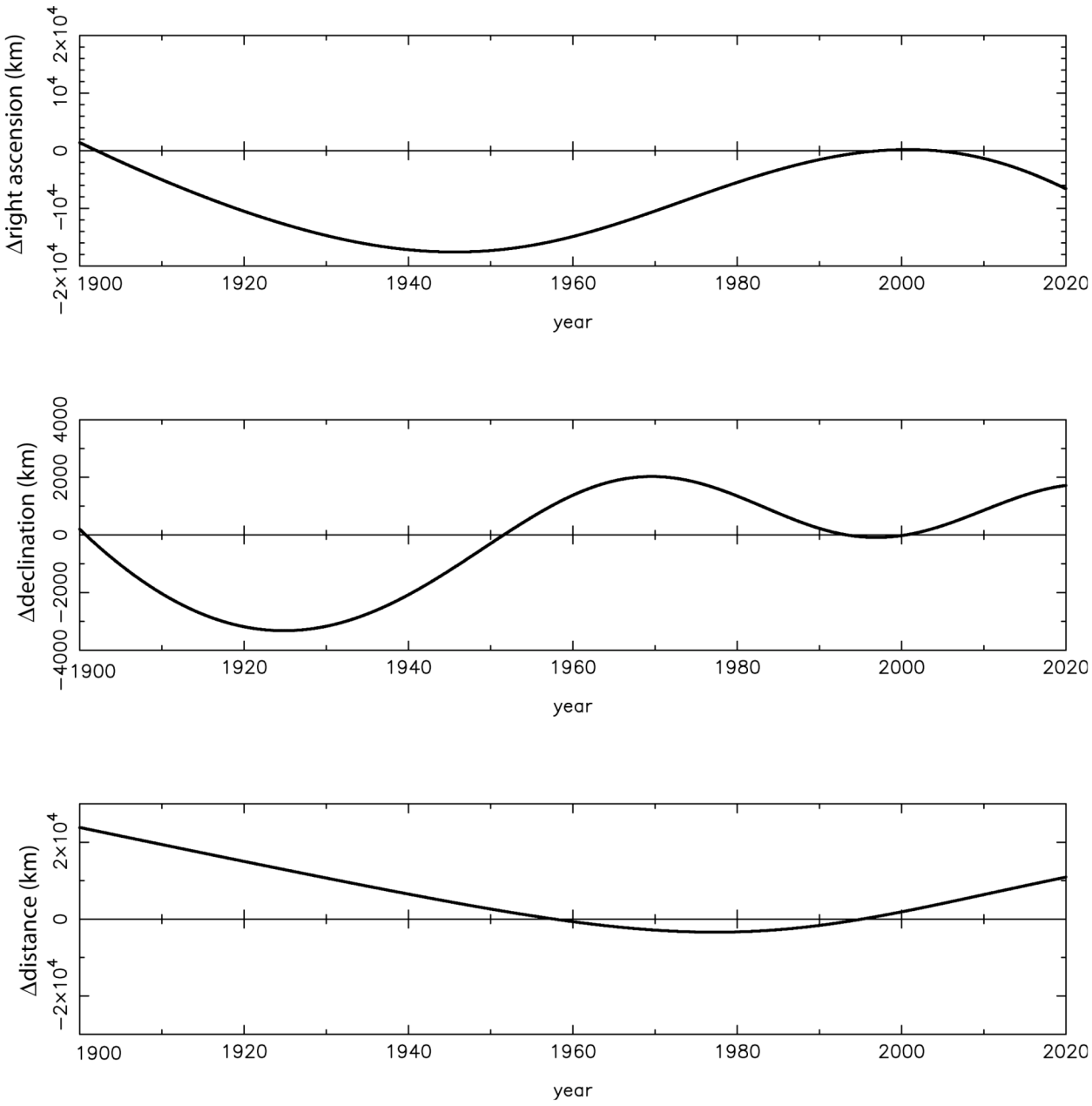

Figure 14: Difference in Pluto orbit, relative to the solar system barycenter, between DE418 and DE414.

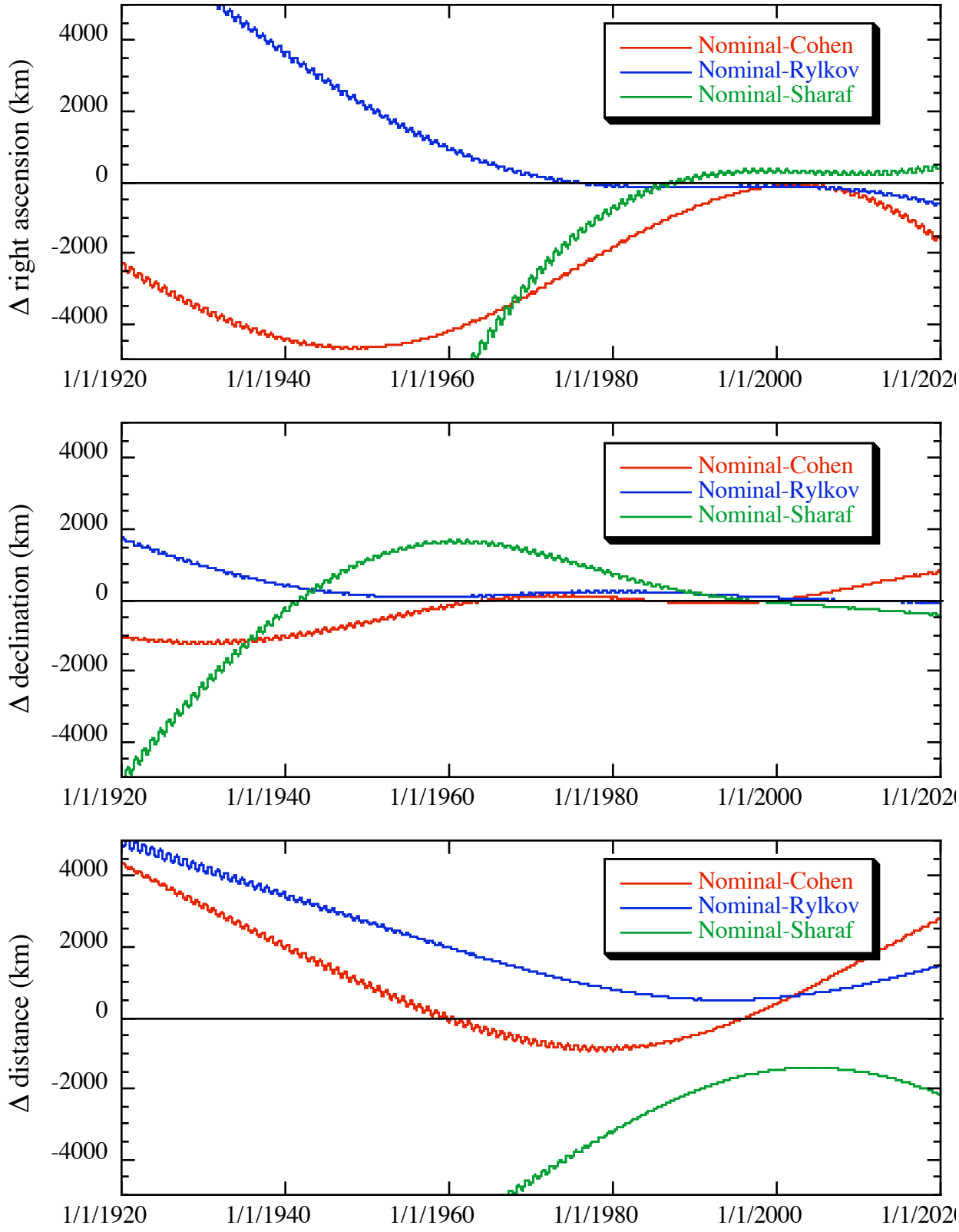

Figure 15: Differences between the DE418 orbit of Pluto and three test ephemerides estimated with different data sets.

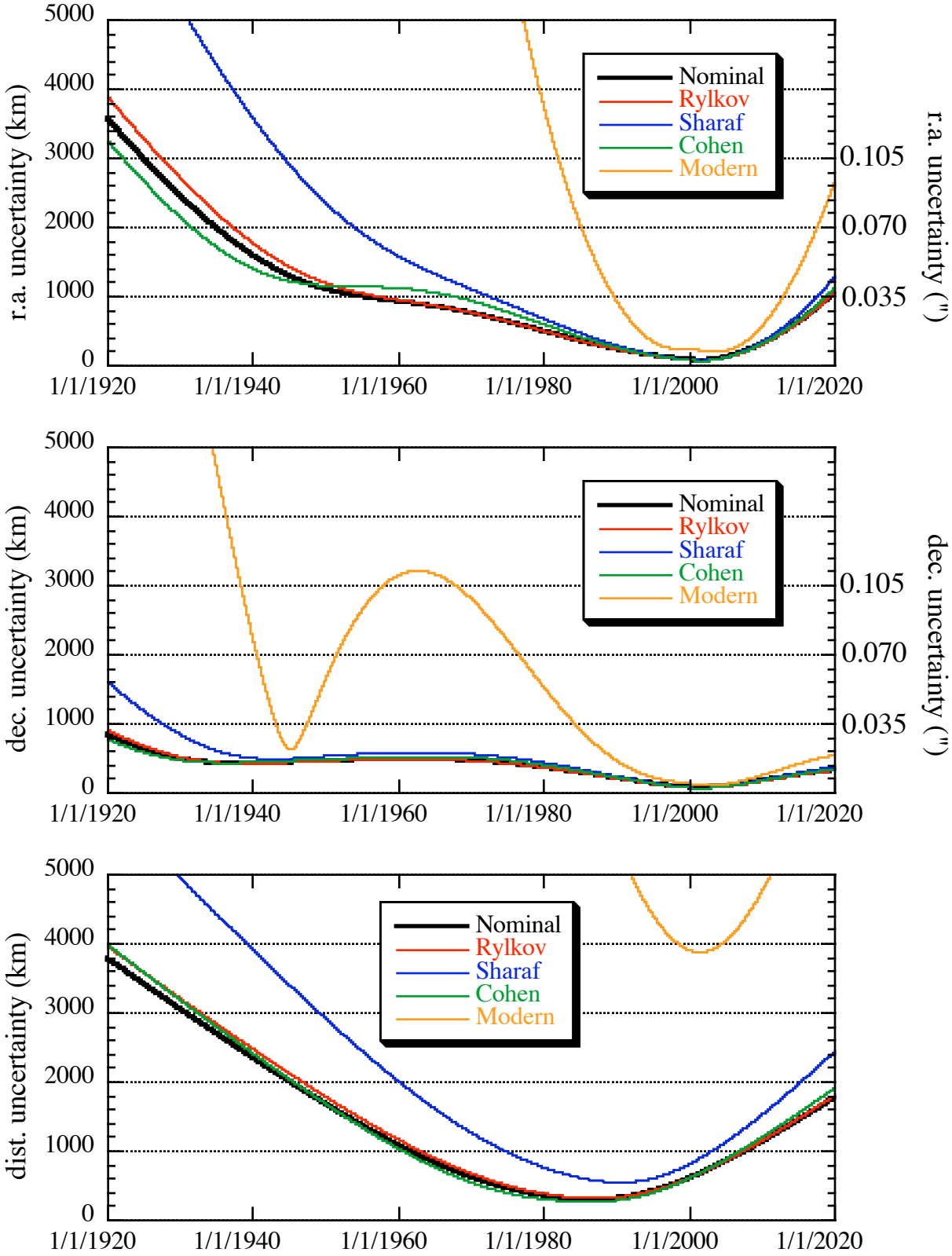

Figure 16: Formal estimated uncertainty in Pluto position components based on different data sets.

Table 2 Recommended Pluto orbit covariance for New Horizons encounter in 2015 in ODP input format with units of radians^2

```
  APCNAME9(  1) = 'DMW9','DP9','DQ9','EDW9','DA9','DE9',
$
  APCSCALE9( 1) = 6*1.00D+00,
$
  APCOV9( 1,  1) =
    5.681262040816D-13,
  APCOV9( 1,  2) =
   -1.104708737073D-16,    2.158610917637D-14,
  APCOV9( 1,  3) =
   -8.979005669148D-16,    1.253963756493D-14,    8.507943854533D-15,
  APCOV9( 1,  4) =
   -4.717128641070D-14,   -2.122398964128D-16,    2.108666791279D-16,
    7.935917809419D-14,
  APCOV9( 1,  5) =
    8.925818447955D-13,    3.440596406743D-16,   -1.669632678538D-15,
   -2.419853645755D-13,    1.781109037141D-12,
  APCOV9( 1,  6) =
    6.141825001181D-13,    2.781880980251D-16,   -1.120941451978D-15,
   -1.737708760759D-13,    1.246279461121D-12,    8.770186882381D-13,
```

Table 3 Recommended Earth orbit covariance for New Horizons encounter in 2015 in ODP input format with units of radians^2

```
  APCNAME3(  1) = 'DMWB','DPB','DQB','EDWB','DAB','DEB',
$
  APCSCALE3( 1) = 6*1.00D+00,
$
  APCOV3( 1,  1) =
    6.8807833589D-19,
  APCOV3( 1,  2) =
    7.9953844334D-20,  1.4390758049D-18,
  APCOV3( 1,  3) =
   -2.6628201996D-19, -1.2525961876D-19,  1.0306123338D-18,
  APCOV3( 1,  4) =
    6.3325275848D-21,  1.6052535550D-21, -4.4769401096D-21,  1.7786672634D-22,
  APCOV3( 1,  5) =
    6.9393589511D-22, -1.0163282243D-23,  2.6259543384D-23, -4.0558797719D-24,
    2.0968775384D-24,
 APCOV3( 1,  6) =
   -2.5230104508D-21, -1.5633954387D-22, -3.0305920494D-22,  1.5684301292D-24,
   -7.5720670170D-24,  7.7090512387D-23,
```

References

Anderson, J. D., Colombo, G., Esposito, P. B., Lau, E. L., Trager, G. B., The mass, gravity field, and ephemeris of Mercury, Icarus, 71, 337-349, 1987.

Barbieri, C., Capaccioli, M., Ganz, R., Pinto, G., Accurate positions of the planet Pluto in the years 1969-1970, Astron. J., 77, 521-522, 1972.

Barbieri, C., Capaccioli, M., Pinto, G., Accurate positions of the planet Pluto in the years 1971-1974, Astron. J., 80, 412-414, 1975.

Barbieri, C., Pinocchio, L., Capacciloi, M., Pinto, G., Schoenmaker, A. A., Accurate positions of the planet Pluto from 1974 to 1978, Astron. J., 84, 1890-1893, 1979.

Barbieri, C., Benacchio, L., Capacciloi, M., Gemmo, A. G., Accurate positions of the planet Pluto from 1979 to 1987", Astron. J., 96, 396-399, 1988.

Cohen, C. J., Hubbard, E. C., Oesterwinter, C., New orbit for Pluto and analysis of differential corrections, Astron. J., 8, 973-988, 1967.

Elliot, J., The center of light of the Pluto-Charon system, private communication, 2002

Fairhead, L.., Bretagnon, P., An analytical formula for the time transformation TB-TT, Astron. Astrophys., 229, 240-247, 1990.

Gemmo, A. G., Barbieri, C, Astrometry of Pluto from 1969 to 1989, Icarus 108, 174-179, 1994.

Folkner, W. M., Uncertainty in the orbits of Earth and Mars for MSL planning, JPL IOM 343R-06-003, 2006.

Jacobson, R. A., Jovian satellite ephemeris JUP230, private communication, 2005.

Jacobson, R. A., The orbits of the satellites of Pluto PLU017, private communication, 2007.

Jacobson, R. A., Riedel, J. E., Taylor, A. H., The orbits of Triton and Nereid from spacecraft and Earth-based observations, Astron. Astrophys., 247, 565-575, 1991.

Jacobson, R. A., Campbell, J. K., Taylor, A. H., Synnott, S. P., The masses of Uranus and its major satellites from Voyager tracking data and Earth-based Uranus satellite data, Astron. J., 103, 2068-2078, 1992.

Jacobson, R. A., Antreasian, P. G., Bordi, J. J., Criddle, K. E., Ionasescu, R., Jones, J. B., Mackenzie, R. A., Pelletier, F. J., Owen, W. M. jr., Roth, D. C., Stauch, J. R., The gravity field of the Saturnian system from satellite observations and spacecraft tracking data, Astron. J., 132, 2520-2526, 2006.

Jensen, K. S., Accurate astrometric positions of Pluto, 1975-1978, Astron. Astrophys. Suppl., 36, 395-398,1979.

Klemola, A. R., Harlan, E. A., Astrometric observations of the outer planets and minor planets: 1980-1982, Astron. J., 87, 1242-1243, 1982.

Klemola, A. R., Harlan, E. A., Astrometric observations of the outer planets and minor planets: 1982-1983, Astron. J., 89, 879-881, 1984.

Klemola, A. R., Harlan, E. A., Astrometric observations of the outer planets and minor planets: 1984-1985, Astron. J., 92, 195-198, 1986.

Konopliv, A. S., The lunar gravity field LP150Q, private communication, 2006.

Konopliv, A. S., Banerdt, W. B., Sjogren, W. L., Venus gravity: 180th degree and order model, Icarus, 139, 3-18, 1999.

Konopliv, A. S., Banerdt, W. B., Sjogren, W. L., Venus gravity: 180th degree and order model, Icarus, 139, 3-18, 1999.

Konopliv, A. S., Yoder, C. F., Standish, E. M., Yuan, D., Sjogren, W. L., A global solution for the Mars static and seasonal gravity, Mars orientation, Phobos and Deimos masses, and Mars ephemeris, Icarus, 182, 23-50, 2006.

Lyard, F., Lefevre, F., Letellier, T., Francis, O., Modeling the global ocean tides: insights from FES2004, Ocean Dynamics, 56, 394-415, 2006.

Moyer, T. D., Formulation for observed and computed values of Deep Space Network data types for navigation, Monograph 2, Deep Space Communications and Navigation Series, Jet Propulsion Laboratory/California Institute of Technology, 2001.

Owen, W. M., Observations of the outer planets from Table Mountain Observatory, private communication 2006.

Rapaport, M., Teixeira, R., Le Campion, J. F., Ducourant, C., Camargo, J. I. B., Benevides-Soares, P., Astrometry of Pluto and Saturn with the CCD meridian instruments of Bordeaux and Valinhos, Astron. Astrophys., 383, 1054-1061, 2002.

Ray, R., Tidal spherical harmonic coefficients for FES2004 Mf, http://bowie.gsfc.nasa.gov/ggfc/tides/harm_fes04.html, 2006.

Rylkov, V. P., Vityazev, V. V., Dementieva, A. A., Pluto: an analysis of photographic positions obtained with the Pulkovo normal astrograph in 1930-1992, Astronomical and Astrophysical Transactions, vol. 6, pp. 251-281, 1995

Schwan, H., Systematic relations between the Hipparcos catalogue and major (fundamental) catalogues of the 20th century (Paper II), Astron, Astrophys., 373, 1099-1109, 2001

Sharaf. Sh. G., Budnikova. N. A., Theory of the motion of the planet Pluto, Trans. Inst. Theoretical Astronomy, 10, 1-173, 1964 (NASA Technical Translation F-491, 1969).

Standish, E. M., JPL planetary ephemeris DE 414, JPL IOM 343R-06-002, 2006.

Standish, E. M., Newhall, X X, Williams, J. G., Folkner, W. M., JPL Planetary and lunar ephemeris DE403/LE403, JPL IOM 31410-127, 1995.

Stone, R. C., Monet, D. G., Monet A. K. B., Harris, F. H, Ables, H. D., Dahn, C. C., Canzian, B., Guetter, H. H., Harris, H. C., Henden, A. A., Levine, S. E., Luginbuhl, C. B., Munn, J. A., Pier, J. R., Vrba. F. J., Walker, R. L., Upgrades to the Flagstaff astrometric scanning transit telescope: a fully automated telescope for astrometry, Astron. J., 126, 2060-2080, 2003.

Zappala, V., de Sanctis, G., Ferreri, W., Astrometric observations of Pluto from 1973 to 1979, Astron. Astrophys. Suppl., 41, 29-31, 1980.

Zappala, V., de Sanctis, G., Ferreri, W., Astrometric positions of Pluto from 1980 to 1982, Astron. Astrophys. Suppl., 51, 385-387, 1983.

Revision Notes:

The GM for Mars in Table 1 was incorrectly listed as the value on the satellite ephemeris file MAR063; the correct value is from the Mars gravity field of Konopliv et al. The original version of the Pluto orbit covariance in Table 2 was not correctly scaled to radians^2, and has been corrected here. The covariance for the Earth-Moon barycenter in Table 3 had included a row for the covariance on one Mars orbital parameter, which has been removed.

Acknowledgement
The research described in this paper was carried out at the Jet Propulsion Laboratory, California Institute of Technology, under a contract with the National Aeronautics and Space Administration.